

## Knots in Macromolecules in Constraint Space

Michael Brill, Philipp M. Diesinger, and Dieter W. Heermann

Institut für Theoretische Physik

Universität Heidelberg

Philosophenweg 19

D-69120 Heidelberg

and

Interdisziplinäres Zentrum

für Wissenschaftliches Rechnen

der Universität Heidelberg

(Dated: October 2, 2018)

## Abstract

We find a power law for the number of knot monomers with an exponent  $0.39 \pm 0.13$  in agreement with previous simulations. For the average size of a knot we also obtain a power law  $N_m = 2.56 N^{0.20 \pm 0.04}$ . We further present data on the average number of knots given a certain chain length and confirm a power law behaviour for the number of knot monomers. Furthermore we study the average crossing number for random and self-avoiding walks as well as for a model polymer with and without geometric constraints. The data confirms the  $aN \log N + bN$  law in the case of without excluded volume and determines the constants  $a$  and  $b$  for various cases. For chains with excluded volume the data for chains up to  $N = 1500$  is consistent with  $aN \log N + bN$  rather than the proposed  $N^{4/3}$  law. Nevertheless our results show that the  $N^{4/3}$  law is a suitable approximation.

PACS numbers:

Keywords: knots, biopolymers, polymers, constraint space, statistical physics, Monte Carlo simulation, average crossing number

## I. INTRODUCTION

Knots are of biological interest because they preserve topological information. In DNA packing and unpacking, an enzymatic reaction converts DNA strands to knots. Such knots are actively removed under energy consumption from ATP, by topoisomerase II by cutting a DNA segment, passing another segment through the gap, and resealing the cut of the former, until eventually the topology of the chain is that of an unknot. In bacteria DNA occurs knotted, i.e. in a state topologically different from a simply connected ring. This can be seen using electron microscopes. Underlying and overlying segments are distinguished using a protein coating. The attenuated DNA is then visualized as a knot. The unknotting number and ideal crossing number can then be estimated. For several DNA fragments with the same knot number there may be a variety of different forms as the DNA is twisted and distorted. However, the average writhe and crossing number can be estimated for a particular ideal knot number. A more convenient procedure for determining the crossing number of DNA knots involves using gel electrophoresis.

It has been shown that DNA knots having the same molecular size increase their speed of electrophoretic migration with increasing number of nodes, i.e. the intersections of DNA segments in planar projections<sup>1</sup>. However, these early gel systems did not succeed in separating different DNA knots with the same minimal crossing number. It is a key question to understand the statistical behaviour of such knotted DNA to understand a number of physiological processes having to overcome this knottedness, or to quantify results from DNA separation techniques such as electrophoresis, in which the knottedness influences the mobility.

DNA in restricted volumes shows knots, for example when linear double-stranded DNA is packed inside bacteriophage capsids. For such a situation the knotting probabilities of equilateral polygons confined into spherical volumes were calculated by Monte Carlo simulations<sup>2</sup>.

Already a random walk (the DNA might be considered in some circumstances as a random walk) can frequently lead to the formation of knots and it was conjectured (Frisch-Wasserman-Delbruck conjecture<sup>3,4</sup>) and proven that as the walk becomes very long the probability of forming nontrivial knots upon closure of such a walk tends to one<sup>5,6,7</sup>. In thermally fluctuating long linear polymer chains in solution, the ends come from time to

time into a direct contact or at close vicinity of each other. At such an instance, the chain can be regarded as a closed one and thus will form a knot. Simple knots show their highest occurrence for shorter random walks than more complex knots<sup>8,9</sup>.

How does one identify a knot in a polymer chain? From a mathematical point of view one uses the Alexander-Jones polynomial or other types of invariants, known as knot (or link) polynomials and defined via skein relations<sup>10,11,12,13,14</sup>, i.e. a set of rules defining a knot polynomial invariant. The Alexander polynomial is calculated from a two-dimensional projection of a three-dimensional knot. It provides an invariant in as far as all the projections yield the same polynomial. Unfortunately, there are pairs of distinct knots that share the same Alexander polynomial. This is typical in as far as the invariants in general are not one-to-one. Since there is no exact algorithm for classifying all knots, in this paper we use a practical approach to the identification of knots. We apply a force to the polymer stretching it. If there is a knot in the chain, it will tighten and can then be identified.

In this paper we take up the question of the statistics and properties of polymers with topological and geometric constraints, in particular those with knots. From a theoretical point of view, the statistical mechanics of such entangled systems is an unsolved problem<sup>15,16</sup>.

As pointed out above, an important concept for the identification of knots and the statistics of them is the average crossing number (ACN). Diao suggested to use the ACN as a measure of entanglement to determine whether a polymer chain (closed) is highly or weakly knotted<sup>6</sup>. For a given linear closed polymer the crossing number associated with a particular projection of the random walk is the number of crossings one observes when the polymer is projected to a plane under the given projection direction. The average crossing number of the polymer is then defined as the average of this crossing number over all possible projection directions<sup>6</sup>.

We note that although a linear DNA behaves like a Gaussian walk up to rather high lengths<sup>17</sup>, at fixed topology even a Gaussian chain behaves like an SAW-chain<sup>18</sup>. Thus we investigate the knots or rather in the corresponding section the average crossing number (ACN) for the case of phantom chains and chains with excluded volume. Both are investigated with and without the constraint of presence of a wall excluding one half space.

For equilateral and for Gaussian random walks Diao<sup>6</sup> succeeded in showing that the average crossing number behaves  $N \log N + cN$ . For self-avoiding chains no analytical result is yet available but a suggestion by Buck<sup>19</sup> that with excluded volume the behaviour changes

to a power law .

In this paper we first consider the average crossing number for the case of random and self-avoiding walks under the constraint that they are attached to a wall. Then we focus on the knot statistics and present results for the statistics of knots. We investigate the average number of the knots given a certain chain length and confirm a power law behaviour for the number of knot-monomers.

## II. THE AVERAGE CROSSING NUMBER

We start by investigating the effects of excluded volume interactions on the average crossing number (ACN) of equilateral and Gaussian random walks (phantom chains) which represent polymer classes. To understand the effect of the excluded volume interaction, let us focus our attention initially on the invariant

$$a(l_1; l_2) = \frac{1}{2} \int_0^Z \int_0^Z \frac{j_1(t); j_2(s); j_1(t) j_2(s)}{k_1(t) k_2(s) k^3} dt ds \quad (1)$$

which is the basis for the prediction<sup>20,21</sup>

$$ACN_{\text{Gaussian}}(N) = \frac{1}{2} N \log(N) + O(N) = \frac{1}{2} N \log(N) + c_1 N \quad (2)$$

$$ACN_{\text{Equilateral}}(N) = \frac{3}{16} N \log(N) + O(N) = \frac{3}{16} N \log(N) + c_2 N \quad (3)$$

for the phantom and equilateral chains of length  $N$  without excluded volume. In the above  $l_1$  and  $l_2$  are segments of the chain and  $s$  is the arclength parametrization. Eq. (1) is a link invariant which specifies the topological state of the polymer which, however, is not of the one-to-one type<sup>22,23</sup> and is not a true invariant for knots<sup>10,24</sup>. While the above invariant does not succeed in uniquely characterizing the knot, it is the first element in a hierarchy.

In<sup>20,21</sup> it was shown that for two chain segments  $l_1; l_2$  on average  $a(l_1; l_2)$  behaves as

$$\langle a(l_1; l_2) \rangle = \frac{1}{2} \frac{1}{d^2} + O\left(\frac{1}{d^{2.5}}\right) \quad (4)$$

for Gaussian phantom and

$$\langle a(l_1; l_2) \rangle = \frac{1}{16} \frac{1}{d^2} + O\left(\frac{1}{d^3}\right) \quad (5)$$

for equilateral phantom chains, where  $d$  is the distance between the two considered chain segments. So far no prediction has been derived for the case of chains with excluded volume interaction. Hence it is important to ask how far the estimate also applies to the case of excluded volume interaction and how differences manifest themselves.

Using Monte Carlo simulation<sup>25,26</sup> we calculated the average crossing number by counting the crossings in numerous projections of  $\mathbf{r}$  and taking the average over all these crossing numbers. For every calculated average crossing number, we averaged over 1000 randomly chosen planes to obtain a good estimate of the actual ACN value.

Four types of chains have been investigated by us: Gaussian and equilateral chains with and without excluded volume. All chains are open and start at the origin. The excluded volume chains were generated using a Pivot-Algorithm, which for example can be found in<sup>27</sup>. We used a hard-core excluded volume potential, in order to speed up the simulations. Between two consecutive chain points there is an ellipsoidal hard-core excluded volume. When generating chains with excluded volume interactions the Pivot-Algorithm simply rejects all chain conformations which have at least two overlapping ellipsoids.

We find that the excluded volume interactions do not have any measurable effect on the behaviour of  $\langle a(l_1; l_2) \rangle$  for distances larger than 10 chain segments, and only a slight one for shorter distances (see Figures 1 to 4). This shows that there are nearly no orientation effects on  $\langle a(l_1; l_2) \rangle$  due to the excluded volume interactions and mainly a dependence on the distance distribution of the chain segments.

The strong reduction of  $E(a(l_1; l_2))$  for chains with excluded volume (see Figure 3) is a result of the altered distance probability density function (pdf) and not of any orientation effects. One can see that the chains with excluded volume are much more stretched as expected due to the enhanced value of  $\langle r^2 \rangle$  for the radius of gyration than those without. As a consequence the total  $\langle a(l_1; l_2) \rangle$  for the chains with excluded volume is much lower than for chains without excluded volume.

The pdf of  $d$  is shown in Figure 1 for equilateral and Gaussian chains of length  $N = 100$  with and without excluded volume. One can see that the chains with excluded volume are much more stretched than those without and that the Gaussian chains are longer than the equilateral ones. The latter is a consequence of the Gaussian probability distribution since the mean length of Gaussian chain segments is about 1.6 and the length of all equilateral chain segments is normalized.

The pdfs of the equilateral chains show peaks at  $d = 2$ . This is a feature of the equilateral chains since the distance of the endpoints of two consecutive line segments is always larger than 0 and smaller than 2. If  $d$  exceeds 2 the probability to find monomers with a distance  $d$  drops immediately. In the case of the equilateral chains with excluded volume the end to end distance of two consecutive line segments is always larger than

$$d_{\min} = \sin \frac{\pi}{3} = 0.66 \quad \text{with} \quad \pi = 83.62^\circ$$

This can be seen in Figure 1, too: The pdf of the equilateral chains with excluded volume has two discontinuity points (at  $d_{\min} = 0.66$  and  $d = 2$ ). The one without excluded volume shows only the one at  $d = 2$ .

Of course the short range excluded volume effects are the larger ones. In this case  $E(a(d))$  is lowered because more orthogonal orientations are more likely (cf. Figure 4). But there are still long range excluded volume effects, too: Since the orientation of two line segments within a chain with excluded volume slightly depends on all other segments of the chain the excluded volume chains have another pdf as those without excluded volume and this means that the relative orientation of two line segments is altered too. But this effect is very small and can only be seen for equilateral chains (cf. Figure 1). Since the Gaussian chain segments have a distributed length, orientation effects due to long range excluded volume interactions could not be found in this case.

The fact that the ACN via  $\langle a(l_1; l_2) \rangle$  mainly depends on the distance probability density function  $p_N(d)$  and to a much lesser degree on orientation effects can be used to give a rough approximation for the ACN. The number of crossings of a chain of length  $N$  is given by

$$C(N) = \sum_{i=1}^{N-2} (N-i) = \frac{(N-1)(N-2)}{2} \quad (6)$$

$$= \frac{N^2}{2} - \frac{5}{2}N + 3 \quad (7)$$

Now one can use the distance probability density function  $p_N(d)$  as a weight for  $\langle a(d) \rangle$  to obtain an approximation for the ACN

$$\text{ACN} \approx \int_0^Z \langle a(x) \rangle p_N(x) dx \quad C(N) \quad (8)$$

As these random walks are a model for equilibrated polymers in solution and as these polymers do have excluded volume interactions one should expect a much lower ACN for these polymers than predicted by<sup>20,21</sup>.

The prediction for the ACN by Diao et. al.<sup>20,21</sup> as stated in Eq.(3) are in good agreement with our simulations. Our simulation results confirm these results and we calculated a factor of  $c_2 = 0.3051$  for the equilateral chains and a factor of  $c_1 = 0.2265$  for the Gaussian ones.

Furthermore we found a  $N \log(N) + cN$ -behavior for the chains with excluded volume, too rather than the proposed<sup>19</sup>  $N^{4/3}$  law. The test results are compiled in the following two tables.

chains without excluded volume				
data	t	a	sse	rsquare
equilateral	$(3=16)n \log(n) + an$	-0.3051	445.2619	0.9998
Gaussian	$(1=2)n \log(n) + an$	-0.2265	61.38	1.0000

Gaussian chains with excluded volume				
t	a	b	sse	rsquare
$an^b$	0.03239	1.376	11.6763	0.9986
$(1=2)n \log(n) + an$	-0.5968	{	537.53	0.9349
$an \log(n) + bn$	0.07468	-0.1553	16.3505	0.9980
$ax^{4/3}$	0.0407	{	10.07	0.9988
equilateral chains with excluded volume				
$an^b$	0.06382	1.232	1306.1	0.9952
$(3=16)n \log(n) + an$	-0.9812	{	29987	0.8896
$an \log(n) + bn$	0.03914	0.05466	241.58	0.9991
$ax^{4/3}$	0.03086	{	3606.5	0.9867

### III. KNOTS IN MACROMOLECULES

In this part, we focus on the knots in the chains. When one pulls on one end of a polymer chain with the other end fixed, at a wall for example, it will be stretched. If the force is high enough, the end-to-end-distance distribution should have a large peak at over 95% of

the backbone length. This is the case if the polymer is unknotted, i.e. when it is possible to stretch the chain completely. But if there are one or more knots in the polymer chain, a part of the total possible length is lost! In this case the peak in the end-to-end distribution will be displaced to smaller elongations. Shown in Figure (5) is the end-to-end distribution averaged over ten independently generated chains of length of  $N = 39$ . These chains were sampled for their end-to-end distribution during Molecular Dynamics<sup>25</sup> runs.

One can see two peaks, the larger one is the peak from the unknotted chains in the sample, the smaller one is the peak from the knotted chains. The knots that occurred in these chains were later analysed to be simple "trefoil" knots.

In principle knots are curves with specific properties like average crossing number (as investigated in the previous section) and topology. Here we apply a heuristic approach to the identification of a knot. We employ the notion of polymers with entanglement which can not be reduced to a straight polymer chain. This means that the knots are an effect of the self-avoiding property of the macromolecules and they do only occur when we stretch the chain. We do not want to investigate the topological properties of these chains but rather want to investigate their statistical properties.

First let us see at many knots in polymer chains of a certain length can be found and how many monomers form such knotted places in the chains. The chains we generate can only be in one half space restricted by an infinite wall. At this wall our polymers are fixed with one end, the other end is used to pull on it. To create a starting configuration, we begin with a self-avoiding random walk<sup>26</sup> with the origin at the wall. After this we pull on the free end of the chain. What we obtain is a configuration that looks like a pearl necklace, with the pearls being the entangled regions. We did not use Alexander-polynomials for the knot detection since our focus is on properties like the knot size.

We simulated chains of size  $N$  ranging from 19 segments to 349 segments. The results for the number of knots  $k$  in the chains is shown in Figure 6. We show the probability  $P(k; N)$  for the occurrence of  $k$  knots in a chain of length  $N$ . The longer the chain is the more rapidly decreases the probability for having no knot in the chain. This is consistent with the prove that the probability for having at least one knot in the chain is one if the chain is long enough<sup>5</sup>. The probability for having exactly one knot in the chain goes through a maximum as do all other probabilities for fixed  $k$ . Thus the longer the chain the more likely it is to have several knots in it.



## A . Number of the monomers in a knot

Before we start to investigate the number of monomers in a knot, we have to point out the problems that arise from our knot definition. We consider a blob of monomers that cannot be completely stretched as a knot. In this definition we assume that the polymer can be completely stretched! How large is the force which stretches the polymer? We used a force which is high enough to stretch the polymer such that the knot(s) become tight enough to count only the monomers that really belong to a knot.

In what follows we compare our results to those in the work of Farago, Kantor and Kardar<sup>31</sup>, where knotted polymers were pulled between two parallel walls. This is a difference to our geometry, but when the polymer is stretched, the interactions between the walls and the polymers are negligible. Hence the results of<sup>31</sup> and those of our investigations are comparable.

Let  $n(N)$  be the number of simulated polymers of length  $N$ ,  $k$  the number of knots, and  $n_k(N)$  the number of simulated chains  $N$  with exactly  $k$  knots.  $P(k;N)$  is the relative frequency to find  $k$  knots in a chain of length  $N$ . Further let  $m_i(N)$  be the number of monomers participating in the  $i$ -th simulated polymer of length  $N$ . Then the number of knot-monomers at fixed length  $N$  is

$$M(N) = \sum_{i=1}^{n(N)} m_i(N) \quad (9)$$

In<sup>31</sup> a power law for the number of knot-monomers is predicted

$$M(N)^{k=1} = N^{0.4 \pm 0.1} \quad (10)$$

For this result only chains with one knot were used. Fitting our data to a power law we obtain an exponent  $0.39 \pm 0.13$

$$N_m^{k=1} = 1.25 N^{0.39 \pm 0.13} \quad (11)$$

In Figure 7 the data is shown. The solid line is the fit to the data and the dotted lines are the power laws with the errors predicted by<sup>31</sup>. The scatter is still very large and especially the last data point seems to be an outlier.

If we look at the chains with a number of knots greater than one, we can also fit the data, but only in the two-knot-case reasonable results can be found. Because of the low number of the highly knotted chains the statistic is not good enough for chains with three or more knots. In Figure 8 the results for the two-knot-chains are shown and compared to the  $N^{0.4}$  law from<sup>31</sup>. The fitted power law we obtain in this case is

$$N_m^{k=2} = 2.18 N^{0.37 \pm 0.18}; \quad (12)$$

This result is still close to the  $N^{0.4}$  power law for the one-knot chains.

Averaging over all chains we obtain a stronger dependence on the chain length than in the one or two-knot case. A power law fit yields

$$N_m = 0.0058 N^{1.42 \pm 0.05}; \quad (13)$$

This result is shown in Figure 9 together with the simulation data.

How large are the knots? We averaged over all chains and over all knots (see Figure 10). The average value of the knot size increases rapidly for short chains and saturates. Assuming again a power law behaviour we obtain

$$N_m = 2.56 N^{0.20 \pm 0.04}; \quad (14)$$

#### IV . D I S C U S S I O N

The average crossing number is one way to characterize knots. Our results show that the topological invariant, which is the basis for the prove by Diao and coworker is not influenced by excluded volume interactions. Hence it is still unclear, especially in the light of the inconclusive simulation data, whether the proven law  $N \log N + cN$  for the non-excluded volume case changes to a power law, as suggested by Buck<sup>19</sup>. Much larger chains are needed to clearly discern between the possibilities. A rough estimate shows that we need a decade longer chains. Here the problem is that despite the well developed Pivot algorithm the computation of the excluded volume interaction is so time-consuming that for now it seems to be possible to do such a calculation only expending a truly fair amount of computing resources.

The statistics of knots show a power law behaviour for all of the quantities investigated in this paper. Here once again the gathering of sufficient statistics for the longer chains is difficult to improve. Desirable would be to increase the chain length by a factor of ten to give a good estimate on the corresponding exponents. What is also lacking is a good derivation of the power laws in one framework.

Acknowledgments

We are very grateful to J. Odenheimer and K. Binder for discussions.

---

Electronic address: heermann@tphys.uni-heidelberg.de; URL: <http://wwwcp.tphys.uni-heidelberg.de>

- <sup>1</sup> O. Sundin and A. Varshavsky, *Cell* 21 103 (1980)
- <sup>2</sup> J. Arsuaga, M. Vazquez, S. Trigueros, D.W. Sumners, and J. Roca *PNAS*, 99, 5373 (2002)
- <sup>3</sup> M. Dellbuck Knotting Problems in Biology. *Proceedings of Symposia in Applied Mathematics*, Vol. 14, pp. 5563. Providence: American Mathematical Society. (1962)
- <sup>4</sup> H.L. Frisch and E. Wassenman, *Journal of the American Chemical Society* 83 3789 (1962)
- <sup>5</sup> D.W. Sumners and S.G. Whittington, *J. Phys. A: Math. Gen.* 21, 1689-1694 (1988)
- <sup>6</sup> Y. Diao *Journal of Knot Theory and its Ramifications*, 4 189 (1995)
- <sup>7</sup> N. Pippenger, *Discrete Appl. Math.* 25 273 (1989)
- <sup>8</sup> T. Deguchi and K. Tsurusaki, *J. Knot Theo. Ram.*, 3 321 (1994)
- <sup>9</sup> A. Dobay, P.-E. Sottas, J. Dubochet and A. Stasiak, *Letters in Mathematical Physics*, 55, 239-247, (2001)
- <sup>10</sup> A.V. Vologodskii, A.V. Lukashin, M.D. Frank-Kamenetskii, and V.V. Anshelevich, *JETP*, 39, 1059 (1974)
- <sup>11</sup> A.V. Vologodskii, A.V. Lukashin, and M.D. Frank-Kamenetskii, *JETP*, 40, 932 (1975)
- <sup>12</sup> K. Koniaris and M. Muthukumar *J. Chem. Phys.*, 95, 2873 (1991)
- <sup>13</sup> T. Deguchi and K. Tsurusaki *Phys. Lett. A*, 174, 29 (1993)
- <sup>14</sup> T. Deguchi and K. Tsurusaki *J. Phys. Soc. Japan*, 62, 1411 (1993)
- <sup>15</sup> S.F. Edwards *Proc. Phys. Soc.*, 91, 513 (1967)
- <sup>16</sup> S.F. Edwards. *J. Phys. A (Proc. Phys. Soc.)*, 1, 15 (1968)

- <sup>17</sup> J.F. Mariko and E.D. Siggia, *Macromol.* 28, 8759 (1996)
- <sup>18</sup> J.M. Deutsch, *Phys. Rev. E*, 59, R2539 (1999)
- <sup>19</sup> G. Buck, *Nature* 392 238-239 (1998)
- <sup>20</sup> Diao Y., Ernst C. The Average Crossing Number of Gaussian Random Walks and Polygons – preprint.
- <sup>21</sup> Diao Y., Dobay A., Kusner R.B., Millett K., Stasiak A. 2003 *J. Phys. A: Math. Gen.* 36:11561-11574.
- <sup>22</sup> L.H. Kauffman. *Knots and Physics*. World Scientific, Singapore, (1993)
- <sup>23</sup> C.L. Adams. *The knot book*. Freeman, New York, (1994)
- <sup>24</sup> G. Calugareanu. *Rev. de math. pures et appl.* (Bucarest), 4, 5 (1959)
- <sup>25</sup> D.W. Heermann, *Computer Simulation Methods in Theoretical Physics* 2nd ed., Springer Verlag, Heidelberg, 1990
- <sup>26</sup> K. Binder and D.W. Heermann, *Monte Carlo Simulation in Statistical Physics*, 4-th Edition, Springer, Heidelberg 2002.
- <sup>27</sup> N. Madras and A. Sokal, *J. Stat. Phys.*, 50, 109
- <sup>28</sup> Y. Diao, A. Dobay, R.B. Kusner, K. Millett A. Stasiak *J. Phys. A* 36 11561 (2003)
- <sup>29</sup> S.F. Edwards, *Proc. Phys. Soc.*, 85, (1965)
- <sup>30</sup> Dobay A., Diao Y., Dubochet J. and Stasiak A. Scaling of the average crossing number in equilateral random walks, knots and proteins –preprint.
- <sup>31</sup> O. Farago, Y. Kantor and M. Kardar, *Europhys. Lett.* 60 (1), (2002)

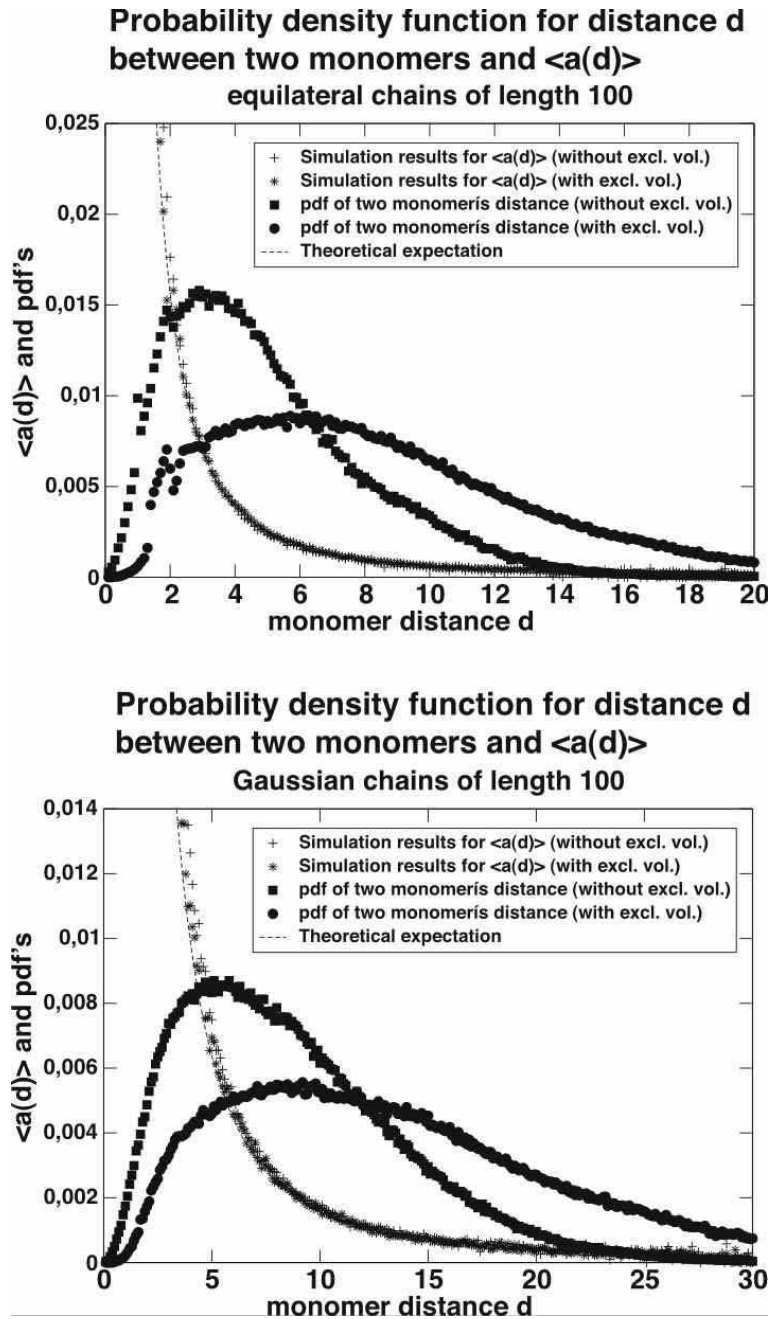


FIG . 1: Shown are the distance probability density functions (pdf) for Gaussian and equilateral chains with the cases of non- and excluded volume. In both cases the distribution is rather different but yield the same behaviour on average (c.f. Figure 2).

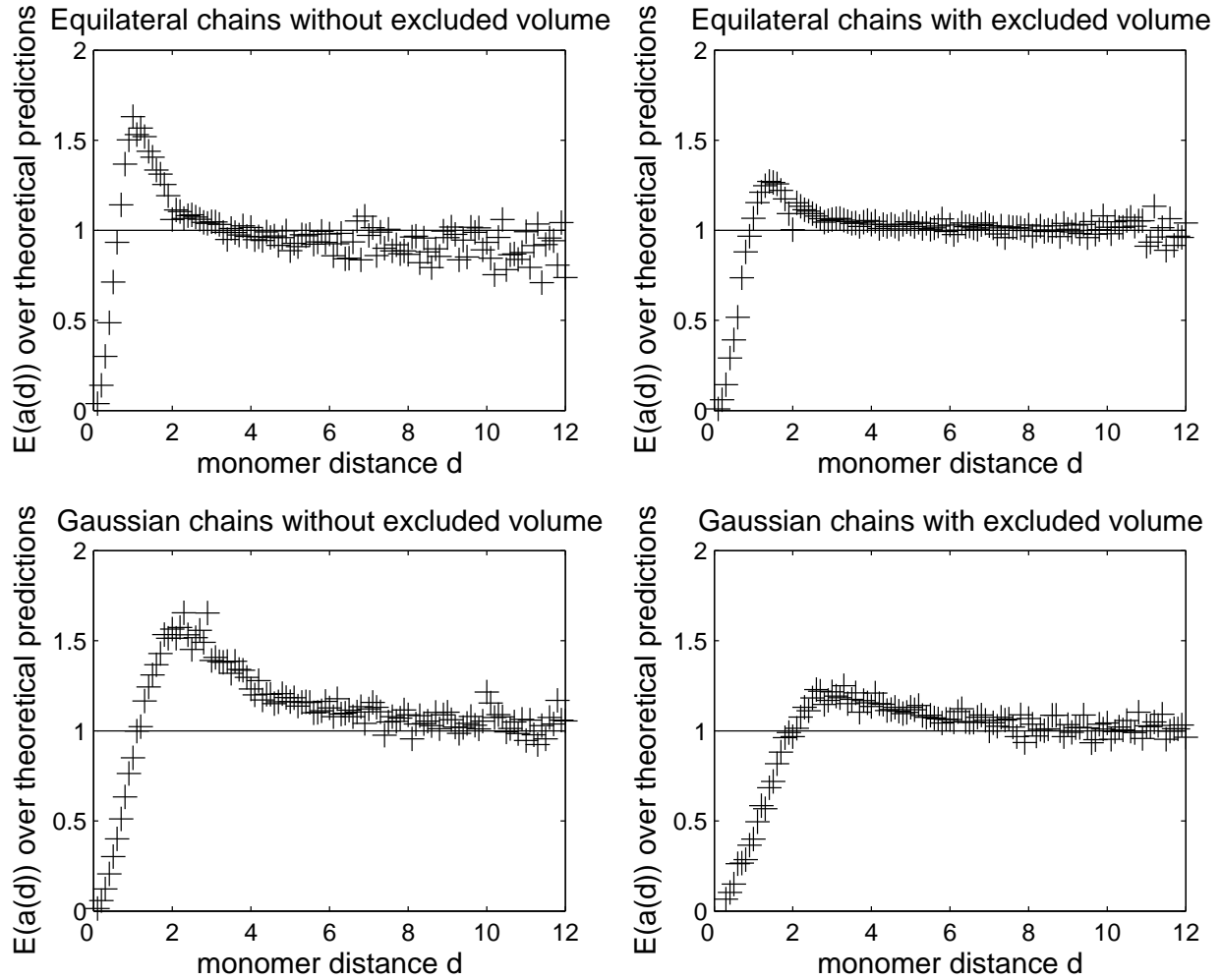


FIG .2: Shown are the ratios between the prediction for the leading order term for the invariant  $a(d)$  characterizing a knot and the simulation results. While the prediction pertains to chains without excluded volume the results show the agreement with the theoretical predictions are excellent for distances larger than 10 for chains with and without excluded volume. The strong fluctuations at the end for the larger distances are a consequence of the plotted ratio. A single point in the figure represents at least averages over 10 000 simulation results.

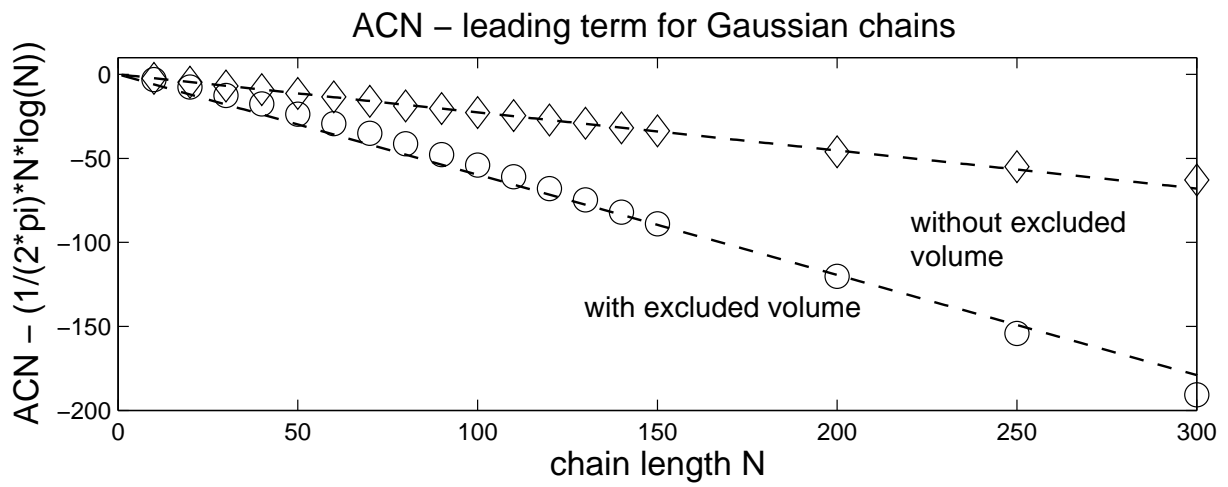
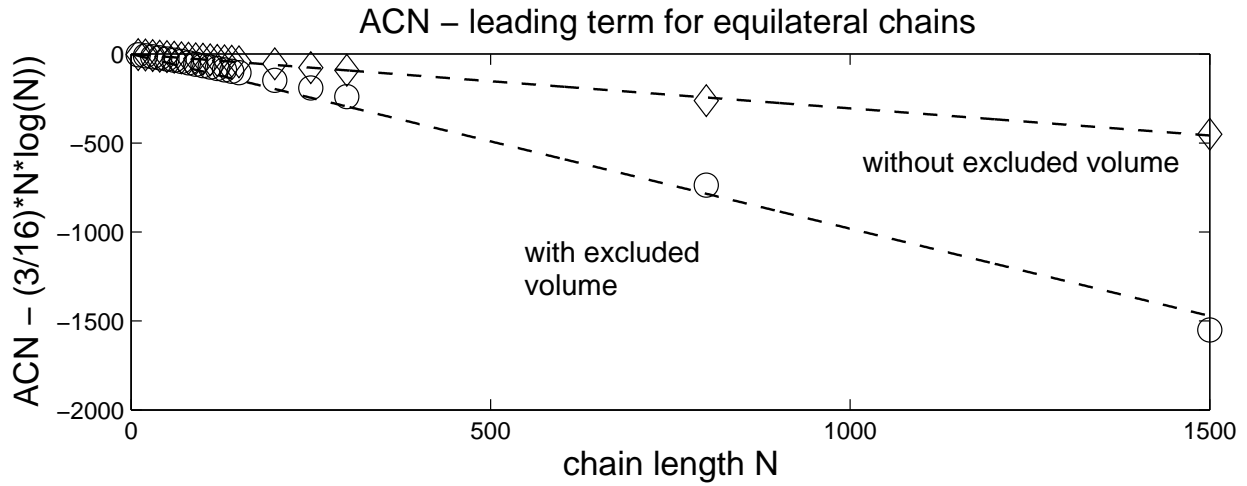


FIG . 3: The error term of the theoretical prediction of the mean average crossing number is negative and much smaller for the chains with excluded volume.

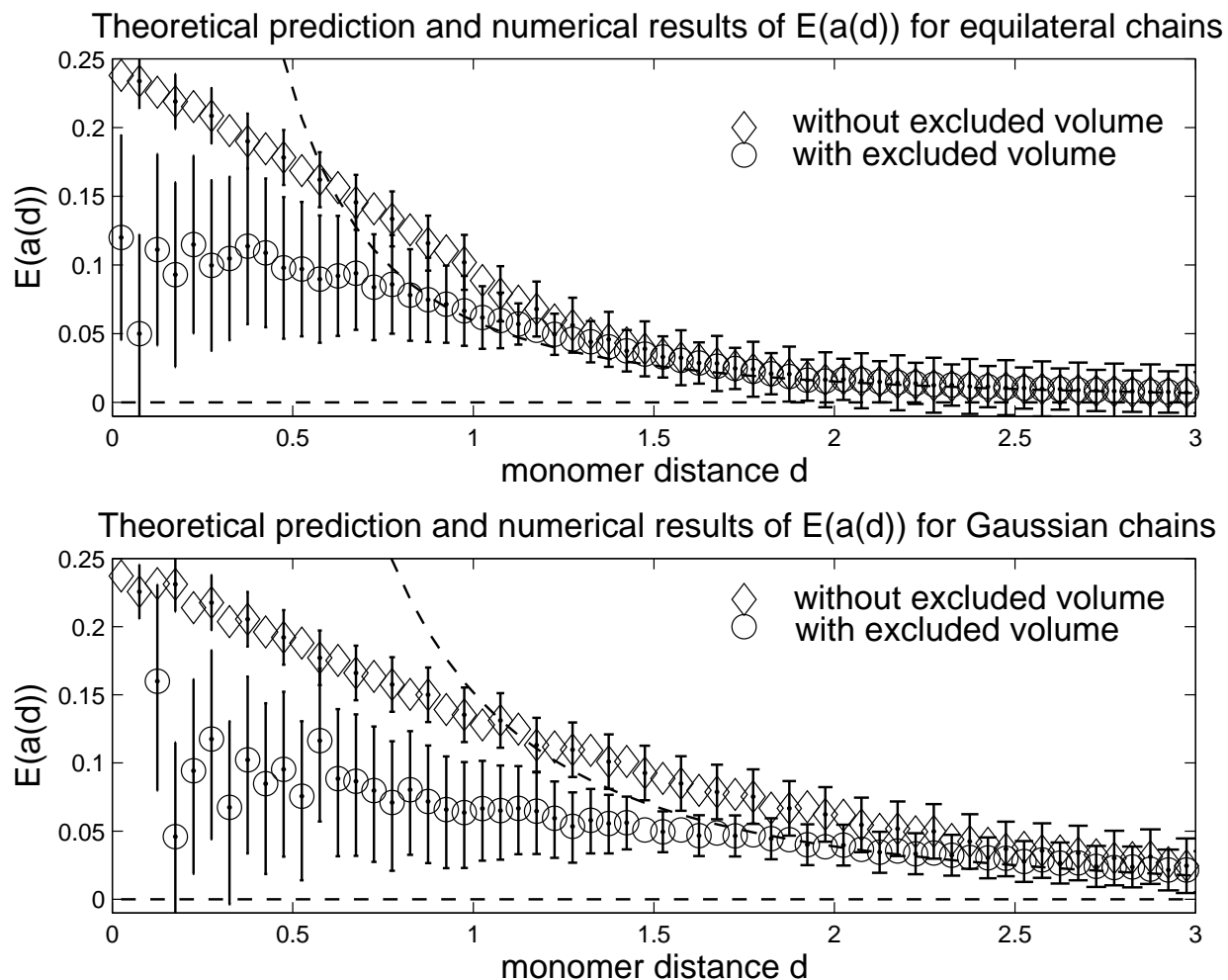


FIG . 4: The theoretical prediction (black line) and the numerical results for  $E(a(d))$  of Gaussian and equilateral chains for small values of  $d$ . One can roughly see that  $E(a(d))$  is discontinuous at  $d = 0$  since  $E(a(0)) = 0$  (cf.<sup>20,21</sup>).



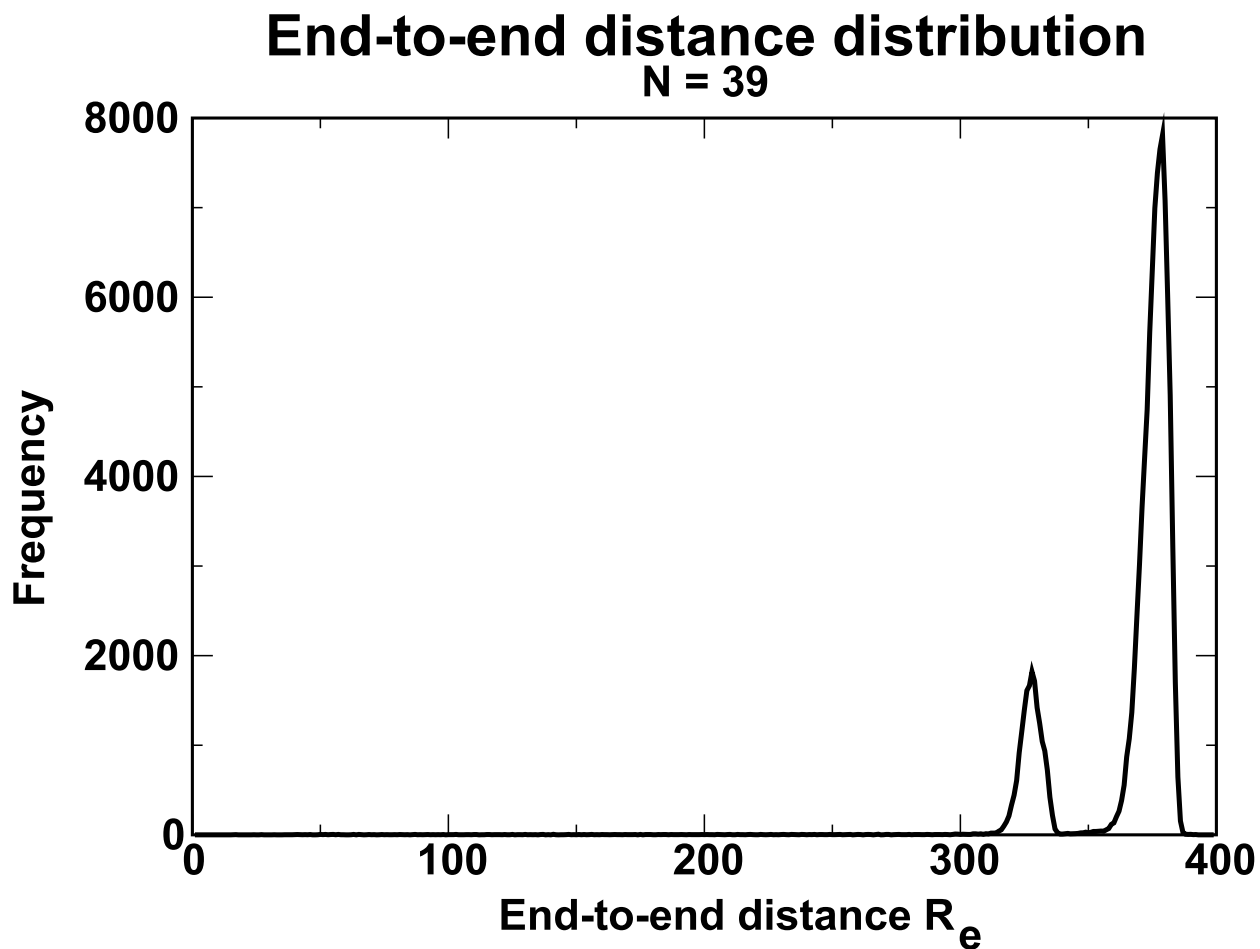


FIG .5: Distribution of the end-to-end distance of chains with and without knots. The plot shows the result of a sample of ten independently generated chains and further sampling was done on these chains for the end-to-end distances. Chains with knots have end-to-end distances in the left peak.

# Probability for the occurrence of a knot

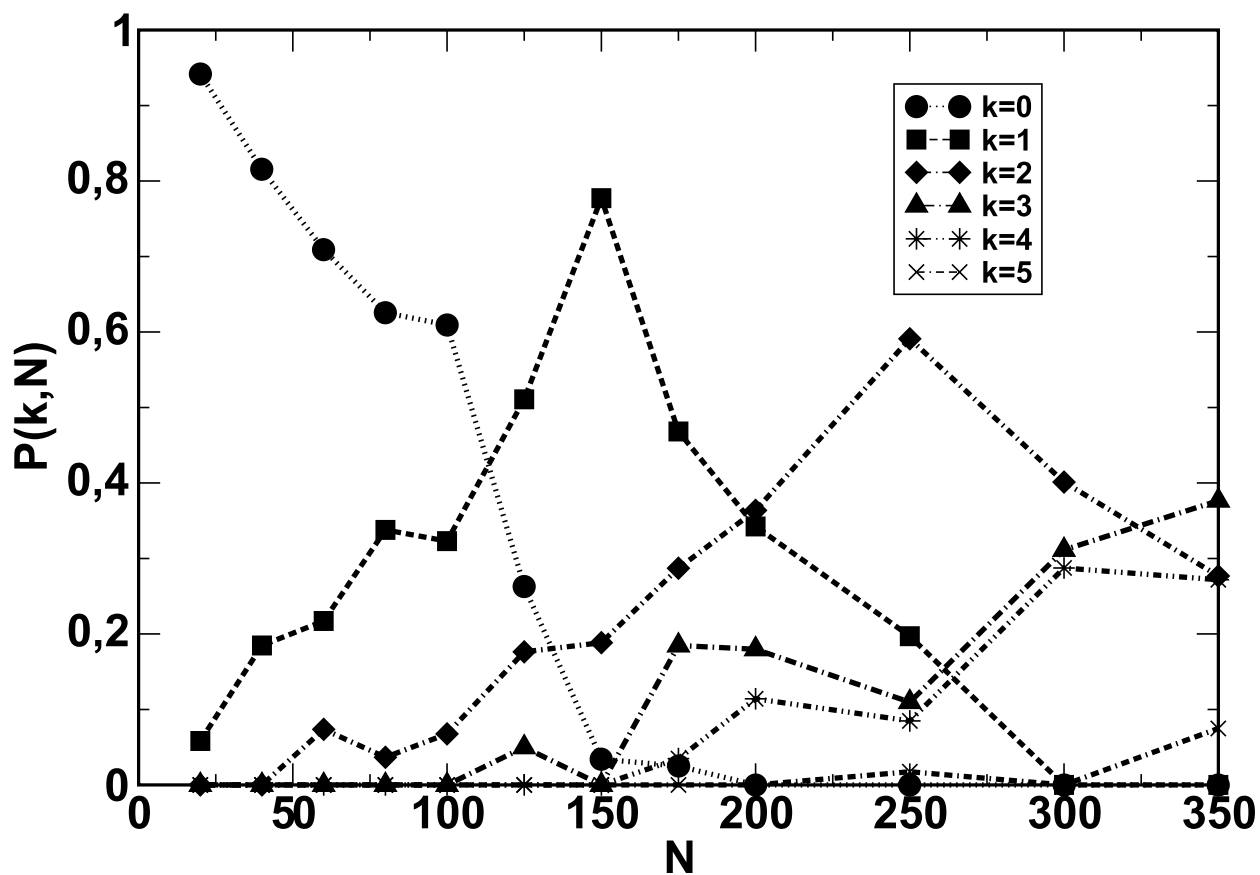


FIG. 6: Shown is the complement of the knot-probability for chains with up to 350 monomers. Shown is that data for chains with up to 5 knots.

# Knot-monomers in chains with one knot

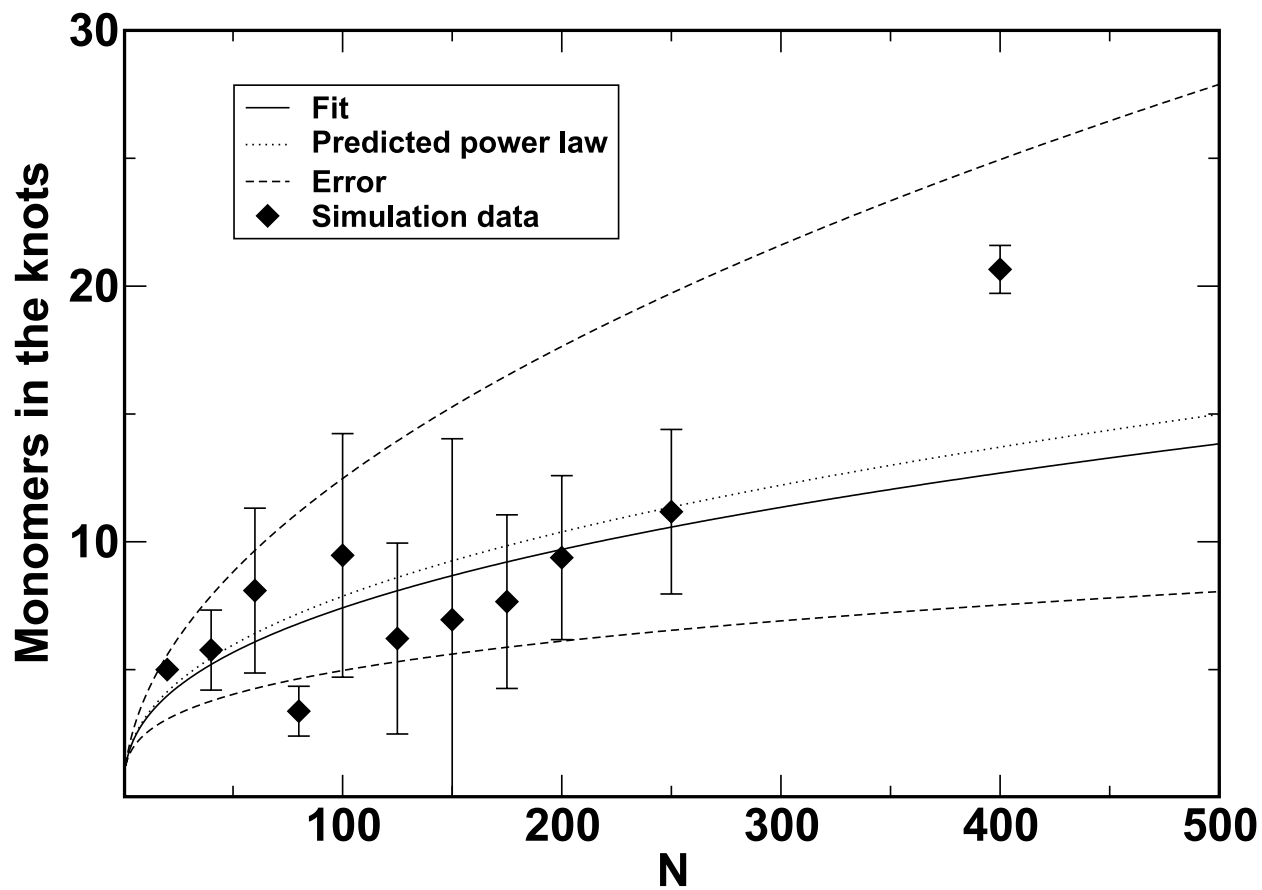


FIG . 7: Number of monomers in the knots in chains with only one knot. The data as well as a calculations by Farago et. al. suggest a power law behaviour with an exponent 0.39.

# Knot-monomers in chains with two knots

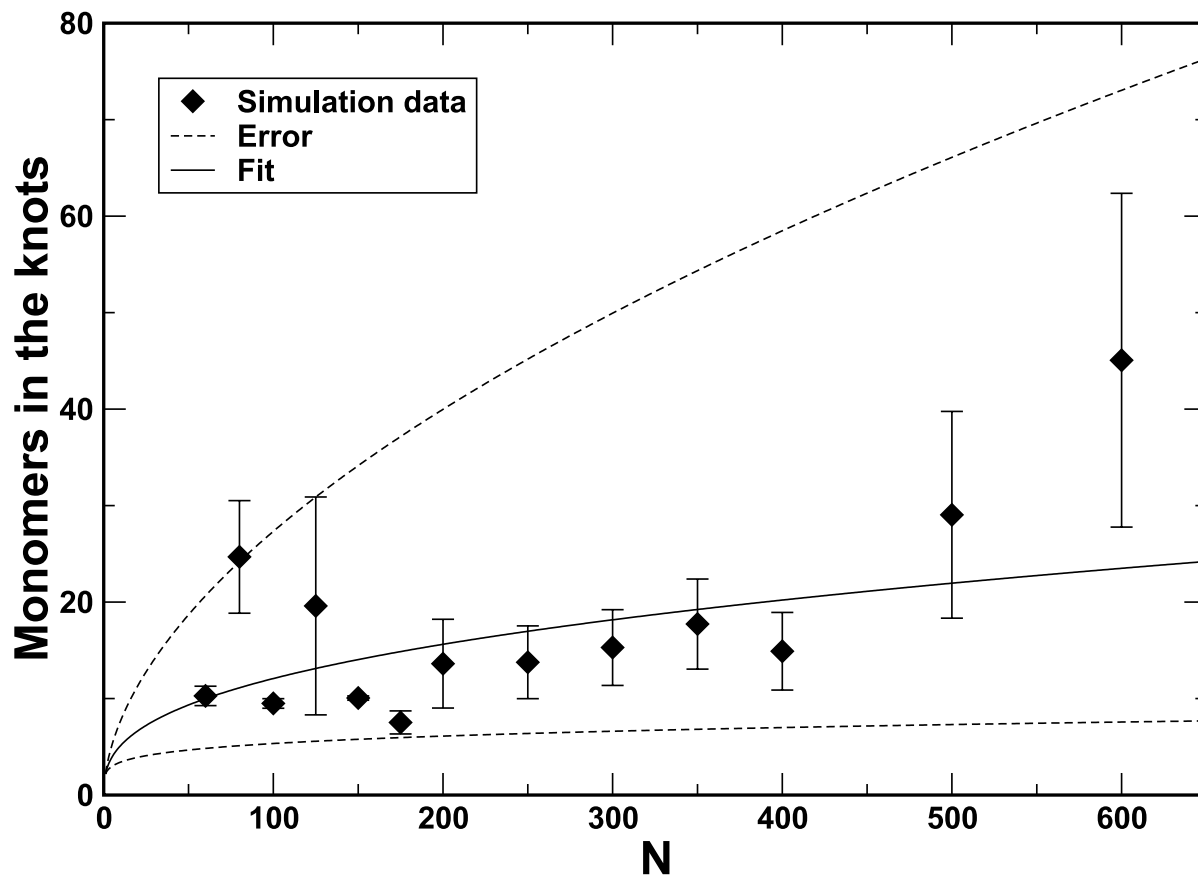


FIG .8: Number of monomers in the knots in chains with two knots. Again we find a power law behaviour with an exponent

# Average number of knot monomers

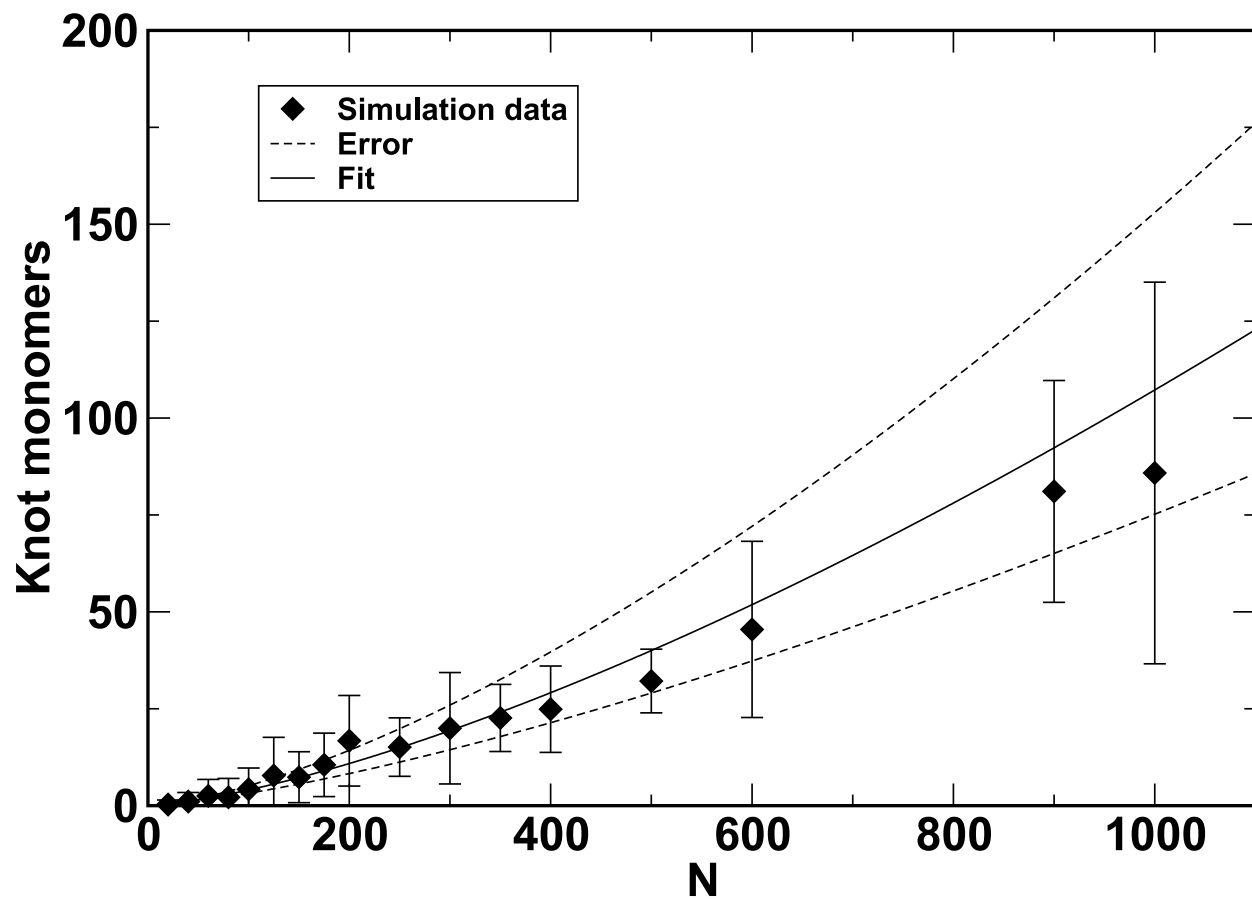


FIG . 9: Number of monomers in the knots. The data suggest a power law behaviour with an exponent 1.42.

# Average knot size

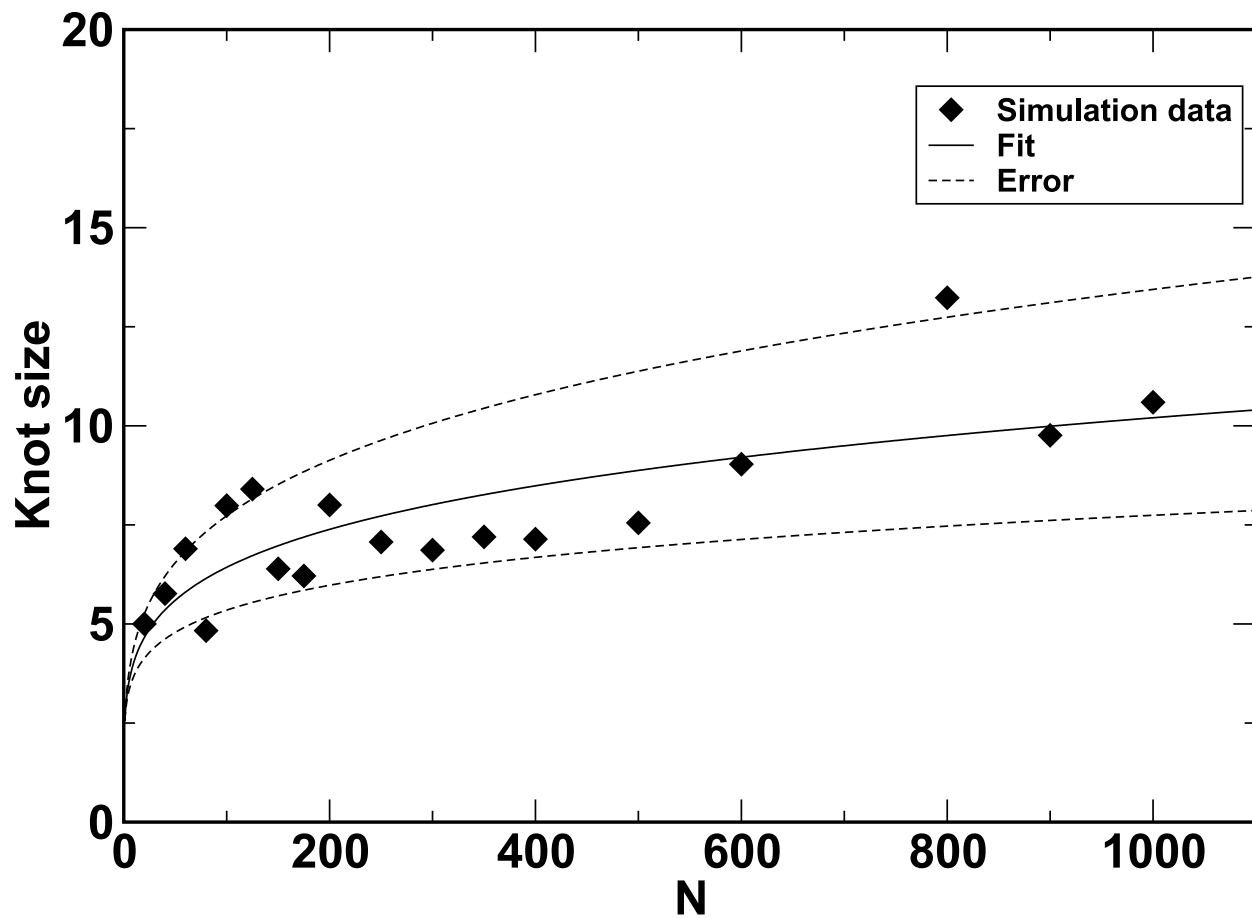


FIG . 10: Average number of monomers in the knots. The plot show a power law fit with an exponent 0.20.